Electric field reconstruction and transport parameter evaluation in CZT X-ray detectors

Electric field reconstruction and transport parameter evaluation in CZT X-ray detectors

M. Pavesi, A. Santi, M. Bettelli, A. Zappettini, and M. Zanichelli

***Abstract*— The laser-induced current technique has been successful used to reconstruct the spatial profile of the electric field along the thickness of a set of CdZnTe spectroscopic X-ray detectors. Current transient profiles for electrons at different applied voltages have been analyzed by means of a minimization procedure demonstrating its applicability to samples with thickness ranging from 250 µm to 4 mm. Mobility and lifetime of electrons have been also deduced and compared with the mobility-lifetime product, as evaluated by fitting the charge collection efficiency curves under a suitable electric field profile model. Comparison between results from both techniques gives a good agreement and confirms the validity of the procedure. This method results applicable each time that carrier transit times can be evaluated from the laser-induced current transients. It could be suitable for many other devices provided that they are made of materials with sufficiently high resistivity, i.e. with a sufficiently low density of free carriers in dark conditions.**

***Index Terms* — II-VI compound semiconductor devices, semiconductor device modeling, X-ray detectors, Laser induced Transient Current Technique (TCT), carrier transport.**

I. INTRODUCTION

The onset of space charge is one of the source of degradation of charge collection efficiency and spectroscopic performances of X- and gamma-ray detectors.

Experimental findings and simulations have shown that the electric field inside CdTe- and CdZnTe-based X-ray detectors is far from the ideal uniform behavior in most of the conditions, showing sometimes non–linear shape [1]-[4]. It is well known that the response of CdTe detectors with rectifying contacts degrades with time when biased under X-ray irradiation as a consequence of the accumulation of negative charge on deep acceptor levels. This phenomenon, known as polarization effect, causes a dramatic worsening in the spectroscopic performance. In some applications, e.g. space telescopes, the flux impinging on the detector is typically very low and a reduction of charge collection efficiency, as a consequence of localized charges, is not acceptable.

Other applications, e.g. medical imaging, require a high photon flux (10^9 photons/s·mm^2) [5], hence detectors with limited space charge accumulation and short charge transit times.

CdTe and CdZnTe crystals show a large concentration of intrinsic defects, if compared with Si or Ge. Although significant work has been done, there remains a lack of fundamental understanding about the identification of electronic defect states and their influence on the collection efficiency and on the charge transport properties [6]-[9].

Space charge inside a bulk detector can be evidenced by the measure of the electric field profile by means of the Pockels effect [1], [2]. An alternative method is the measure of the time of flight of charge carriers crossing the whole detector thickness. The current pulses, induced by the charge generated as a consequence of irradiation with photons or alpha particles, can be fitted to evaluate the two most important transport quantities, mobility μ and lifetime τ. Moreover, some efforts have been spent to reconstruct the electric field from time of flight measurements under the strong assumption of a linear electric field profile [10] or imposing an infinite carrier lifetime [11].

Recently, we have applied a new self-consistent method based on the laser induced Transient Current (TCT) technique to reconstruct the spatial profile of the electric field along the thickness of CdTe photodetectors [12]. The procedure makes possible to extract one by one the transport parameters, mobility μ and lifetime τ, without initial assumption about the electric field profile inside the detector. In addition, this method allows to reconstruct the internal electric field shape simply starting from basic constraints existing among transport quantities and experimental parameters.

In this work, we apply this method for the first time to a set of CZT planar detectors. The interest in this research is twofold. On one side, we demonstrate that is possible to determine at once mobility, carrier lifetime, and electric field profile in CZT samples that show peculiarities regarding transport and trapping mechanisms with respect to CdTe. On the other side, the method is applied in this work to samples with very different sample thickness, ranging from 250 microns to 4 mm, showing that the proposed method is very flexible and applicable to a large range of detectors. It is important to underline that the procedure is applicable whenever the transit time of the charge carrier can be evaluated by the time of flight technique.

II. EXPERIMENTALS

Laser induced current transients have been acquired on a set of planar detectors with thickness ranging from about 250 µm to 4 mm, as reported in Table I. In the following, samples will be named A (270 µm), B (0.5 mm), C (2.5 mm), and D (4 mm). The fitting procedure, described in detail in the next Section, has been applied firstly to estimate mobility and lifetime of electrons. As a second important result, we have reconstructed the electric field profile in the volume of detectors at different biases to check the possible space charge creation, resulting in a distortion of the uniform behavior of the electric field.

Sample	*L* (mm)	Growth Method
A	0.27	VB
B	0.50	THM
C	2.50	VB
D	4.00	VB

Table I. Description of samples and growth methods: Boron Oxide Encapsulated Vertical Bridgman (VB) and Travelling Heater Method (THM).

Making use of a Nd:YAG Polaris II laser system, samples have been optically excited impinging an area of about 500 μm in diameter, at the center of the cathode, with laser pulses at 532 nm, nominally 3 ÷ 4 ns long, and with repetition rate of 20 Hz. The pulse energy is the same for all the acquired current transients. Taking into account of losses along the beam path and of the absorption from the gold contact, the pulse energy released to the material is less than 100 pJ.

Due to the low value of the penetration depth at energies above the energy gap, the pair generation takes place immediately beneath the electrode and the current pulse arises from the drift of only a kind of charge carrier, as well described below. Every induced current pulse has been acquired averaging over a few thousand current pulses: in this way, the out of phase noise contribution and the effect of the little fluctuation of the amount of photogenerated charge by each laser pulse can be further reduced.

The electrodes are thin enough to ensure that the majority of the incoming photons reaches the active region of the detectors. The lateral surface of samples has been shielded to prevent absorption of reflected/diffused light; this is important to prevent unwanted generation of signal at depths other than that just below the metal contact where the laser is focused. The output signals have been amplified by a home-made amplifier with bandwidth of 80 MHz, that ensures a time constant of 2 ns that is comparable with the nominal laser pulse width. The signal is converted into a voltage pulse with a conversion factor of 10^5 V/A and acquired by a Digital Storage Oscilloscope Owon SDS8202, 200 MHz of bandwidth and 2GS/s of sample rate. DC voltage has been supplied by a Keithley 2400 High Voltage Source-Measure Unit. A schematic view of the block diagram for the TCT experiment is shown in Fig. 1.

On the same samples, the Charge Collection Efficiency (CCE) has been measured with excitation at 790 nm from a light source system ORIEL Mod. 66882 suitably screened and focused, consisting in a Quartz Tungsten Halogen-250W lamp, a monochromator CornerStone 130TM 1/8 m Mod. 74000 (wavelength resolution 3 nm), a chopper Signal Recovery Mod. 197 operating at 220 Hz, a lock-in EG&G PARK Mod. 5209. Details about the experimental setup are reported in [13]. All the measurements have been performed in air at room temperature.

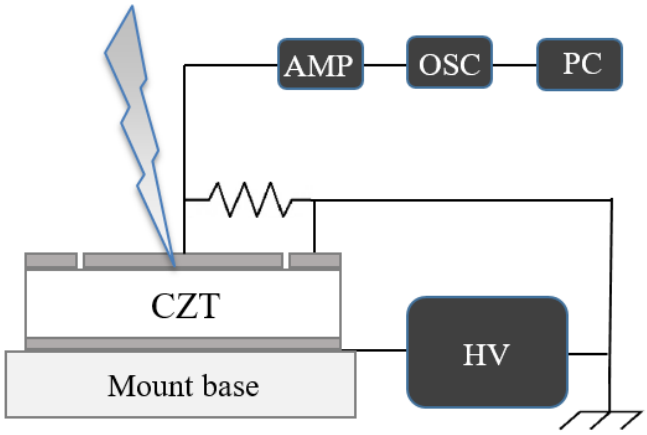

Fig. 1. Schematic view of TCT experiment. Amplification stage is suitably shielded and equipped with a stand-alone electrical supply.

Samples A, C, and D have been cut from 2-inch CdZnTe crystals grown by Boron Oxide Encapsulated Vertical Bridgman [14], [15] with a growth rate of about 1 mm/h and a thermal gradient of 10°C/cm. The starting polycrystalline CdZnTe material has been obtained from 7N elements by direct synthesis [16] and treated at high temperature in order to obtain a charge with reproducible tellurium deviation [17]. The crystals have been grown with Zinc concentration of 10% and Indium doping. A high resistivity has been achieved around 10^{10} Ωcm, as measured by current-voltage (I-V) characteristics at low voltages according to the procedure reported in [18]. Sample B has been cut from a commercial CdZnTe detector. All samples show a surface area of about 7×7 mm^2.

The samples have been mechanically polished with abrasive paper and 0.05 μm alumina suspension, rinsed in methanol, and chemically etched and passivated with a two-step chemical process before the metal contact deposition. Gold contacts have been deposited by electroless procedure. Each detector has been equipped with a central pixel of 5×5 mm^2 area surrounded with a guard ring. During experiments, pixel and guard ring are electrically insulated even if kept at the same potential. Electroless gold contacts show blocking electrical behavior as already reported in our material [19]. All samples selected for TCT measurements (Table I) show good spectroscopic features.

III. PHYSICAL MODEL

The current signal induced by the pulsed laser beam in a detector can be analytically deduced under some simplifying hypothesis: a) the detector has a planar geometry with two opposite electrodes, as depicted in Fig. 1; b) charge carriers are generated primarily in a region close to the illuminated electrode (superficial generation); c) diffusion and detrapping of charge carriers can be neglected; d) carrier mobility and lifetime does not depend on the applied voltage.

When the laser pulse impinges on the cathode of a planar detector, a cloud of charge pairs is generated immediately below the electrode. According to the Ramo-Shockley Theorem (R-S) [20], [21], the main contribution to the induced current is

due to the charge carrier farthest from its collecting electrode (i.e electron if the photons impinge on the cathode). If hypothesis 1) and 2) listed above are fulfilled, the photogenerated signal is then essentially due to a single kind carrier transport. In the following, the case of the signal induced by electrons is discussed. The analytical treatment for holes can be easily deduced.

At fixed voltage V_i, if Q_0 is the photogenerated charge at time $t = 0$ in $x = 0$ (immediately below the metal contact), the electrons move inside the material with a law of motion $x_i(t)$ and die exponentially with a lifetime τ as a consequence of trapping. The index $i = 1,2$ ..,n refers to different values of applied voltage and each of them set a well defined law of motion $x_i(t)$. We can write the electronic density as:

$$n_i(x,t) = Q_0 e^{-\frac{t}{\tau}} \delta\left(x - x_i(t)\right) \qquad (1)$$

where the delta function takes into account the time evolution of the charge density according to the law of motion at each applied voltages.

At time t, the current induced on the anode for the applied voltage V_i can be deduced from the R-S Theorem, introducing the "weighting potential" $w(x) = 1/L$ for a planar detector of thickness L:

$$I_i(t) = \int_0^L e n_i(x,t)\, w(x)\, v_i(x)\, dx = \frac{\mu Q_0 e^{-\frac{t}{\tau}}}{L} E_i\left(x(t)\right) \qquad (2)$$

where $v_i(x(t))$ is the velocity of carrier. At fixed voltage V_i the charge carrier, travelling towards its collecting electrode following the law of motion, experiences the electric field $E_i(x(t))$ in the point $x(t)$ inside the detector. The electric field is related to the carrier velocity from the usual relation $v = \mu E$.

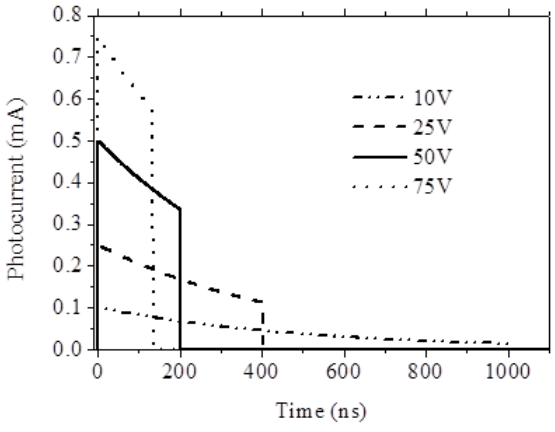

Fig. 2. Current transient profiles calculated from the equation (2) assuming a uniform electric field, L = 0.1 cm, μ = 1000 cm^2/V·s, τ = 500 ns and Q_0 = 0.1 nC.

The photocurrent transients have been calculated for different applied voltages from equation (2) assuming, for example, a uniform electric field profile, L = 0.1 cm, μ = 1000 cm^2/Vs, τ = 500 ns, and Q_0 = 0.1 nC (Fig. 2).

If we reverse the problem, we ask if it is possible to determine the values of Q_0, μ, and τ, starting from curves in Fig. 2. This situation is exactly what happens when we acquire the experimental current transients.

Two physical constraints bind the electric field to the sample thickness and the applied voltage:

$$L = \int_0^{T_{Ri}} v_i\left(x(t)\right) dt = \mu \int_0^{T_{Ri}} E_i\left(x(t)\right) dt \qquad (3)$$

$$V_i = \int_0^{L} E_i(x)\, dx = \mu \int_0^{T_{Ri}} E_i^2\left(x(t)\right) dt \qquad (4)$$

The upper limit in the time integral is the transit time T_{Ri}, defined as the time of flight of the carrier from its generation to the collection at the electrode. Replacing $E_i(x(t))$, as calculated from the equation (2), in the equations (3) and (4) we obtain two relations for each value of applied voltage relating the photogenerated charge Q_{0i} to the temporal profile of the current transients $I_i(t)$. In these relations, the transit times T_{Ri} can be evaluated from curves of Fig. 2, the sample thickness and the applied voltages are known, while we consider the lifetime τ as a free parameter and the mobility μ as an unknown constant quantity:

$$Q_{0i}(\tau) = \int_0^{T_{Ri}} I_i(t)\, e^{+\frac{t}{\tau}} dt \qquad (5)$$

$$\mu Q_{0i}^2(\tau) = \frac{L^2}{V_i} \int_0^{T_{Ri}} \left(I_i(t)\, e^{+\frac{t}{\tau}} \right)^2 dt \qquad (6)$$

The fitting procedure starts choosing a suitable range of values for the lifetime τ and calculating $Q_{0i}(\tau)$ by means of the equation (5) for each value of the applied voltage. The point of intersection of the n generated curves (Fig. 3) is a well-defined value of the lifetime equal to 500 ns for the calculated transients of Fig. 2. This result is not surprising if we assume a generated charge value independent on the applied voltages, resulting as the other coordinate of the point of intersection.

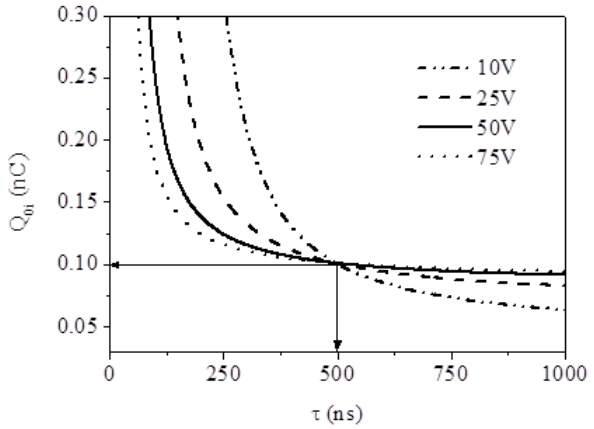

Fig. 3. Photocharge generated at different applied voltages as calculated form equation (5) on varying τ. The intersection point indicates the correct value for Q_0 and τ.

The same approach has been applied to the equation (6), leading to a family of n curves crossing in a point with the

values of μQ_0^2 and τ fixed at the beginning. In this way, the mobility and the lifetime are univocally determined and it becomes possible to know the electric field values experienced by the charge carrier during the motion along the device by means of equation (2). Finally, the law of motion $x(t)$ can be easily obtained and it is possible to reconstruct the spatial profile of the electric field, keeping the time as a parametric variable.

When the above procedure is applied to experimental transients, curves as those in Fig. 3 do not cross in a single point but points of intersection are confined in a very narrow range of values of τ. The choice of the best value for the lifetime will be discussed in the next section.

IV. DISCUSSION AND RESULTS

The procedure described above has been applied to evaluate the transport parameters for electrons in samples listed in Table I. The photocurrent transients have been recorded for each sample at different applied voltages illuminating the grounded cathode. For sake of clarity, only a few selected voltages are shown in Fig. 2. They show a typical behavior consisting in a sharp rise, an intermediate region due to the electronic drift and trapping, and a final diffusion-related tail. In order to calculate the quantities Q_{0i} and μQ_{0i}^2, according to Eqs. (5) and (6), the transit times T_{Ri} have been evaluated from experimental current transients.

The transit times for the calculated curves of Fig. 2 are clearly defined as times at which current pulses drop to zero. The analysis of the experimental curves of Fig. 4 is not so easy and a careful study of the carrier motion has been carried out to choose the correct values for the transit times.

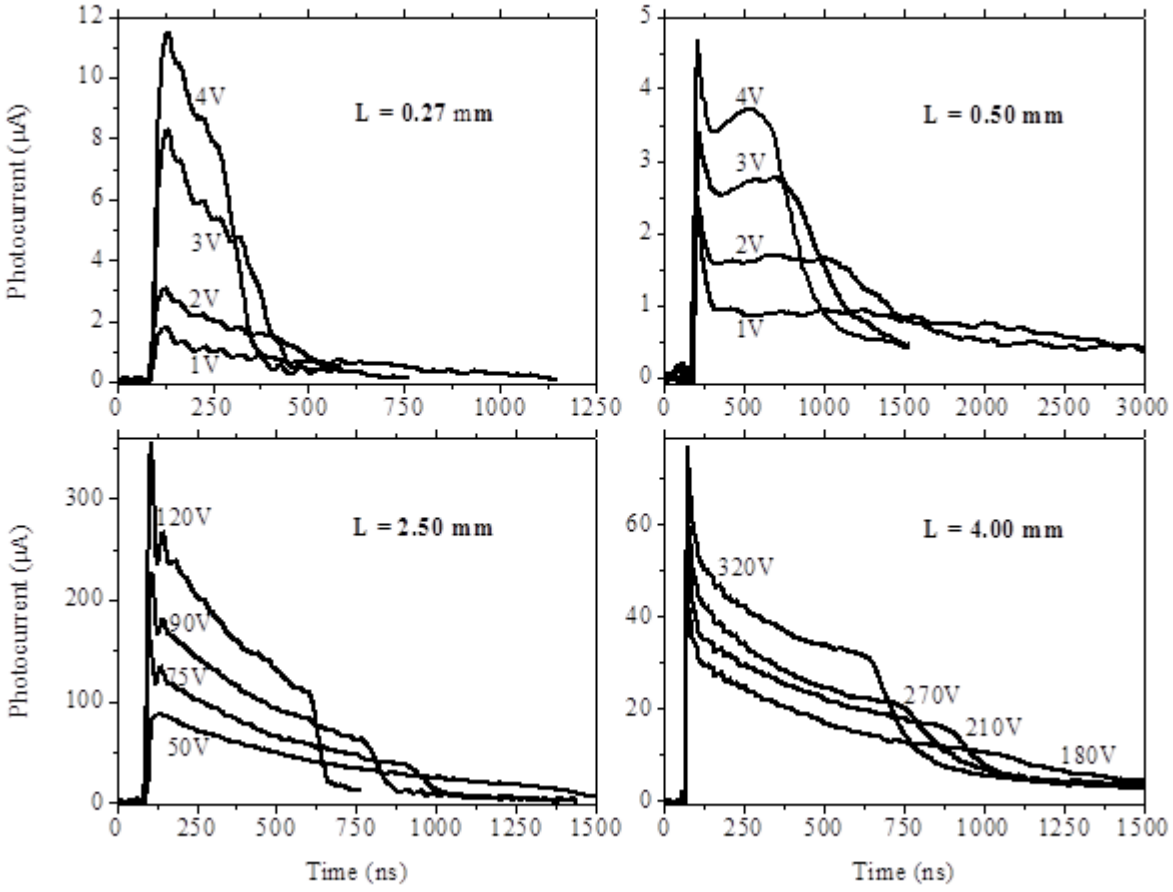

Fig. 4. Photocurrent transients at different applied voltages for samples of Table I.

In the first tens nanoseconds, the photocurrent pulses are highly sensitive to the profile of the laser pulses in time. This is due to the non-instantaneous generation of the carriers due to the finite temporal duration of the laser pulse. To overcome this problem, the current transients have been deconvoluted with the laser pulse shape. In addition, a simulation of drift of the charge cloud in the electric field, under the influence of the thermal diffusion has been carried out, to identify a correct way to evaluate the transit time. Results of this analysis are: a) the edge before the diffusion-related tail is a consequence of the arrival of the first electron to the collecting electrode; b) the charge barycenter starts from the cathode and reaches the anode when

the tail of transient profiles shows a flex point.

After evaluation of the correct transit times from the experimental curves, the first family of curve for the photogenerated charge has been generated from Eq. (5) on varying τ and n points of intersection have been identified.

The uncertainty has been resolved calculating the best value for the electron lifetime τ_1 by minimizing the weighted variance of $Q_{0i}(\tau)$ values. Fig. 5 shows the logarithm function of the variance:

$$Y_1(\tau) = \ln \sum_i \left(\frac{Q_{0i}(\tau) - \langle Q_{0i}(\tau) \rangle}{ErrQ_{0i}(\tau)} \right)^2 \qquad (7)$$

An identical procedure has been applied to equation (6) to calculate $\mu Q_{0i}^2(\tau)$ and then to generate a new family of curves, independent of the previous one. Another best value τ_2 has been obtained by the weighted variance for μQ_{0i}^2, as the minimum of the function $Y_2(\tau)$:

$$Y_2(\tau) = \ln \sum_i \left(\frac{\mu Q_{0i}^2(\tau) - \langle \mu Q_{0i}^2(\tau) \rangle}{Err\,\mu Q_{0i}^2(\tau)} \right)^2 \qquad (8)$$

The dimensionless quantities Y_1 and Y_2, shown in Fig. 5 as a function of τ for the representative sample A, reach a minimum for two well-defined values of the parameter τ (clearly visible in the inset), the average of which is taken as the best value of the electron lifetime. It is noteworthy that an accurate determination of the lifetime requires low voltage measurements, because at high bias the transit time may be lower than the lifetime, introducing an exponentially large error in the determination of carrier lifetime.

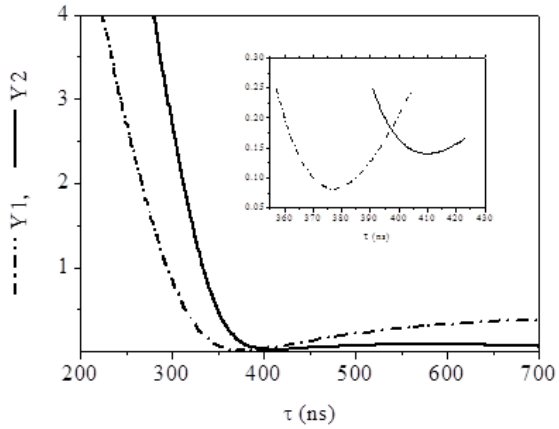

Fig. 5. Minimization procedure: Y_1 and Y_2 calculated as a function of the lifetime τ for the sample A. Inset: zoom of the minima.

At last, the value of the lifetime can be introduced in Eqs. (5) and (6) to calculate the mean value and the standard deviation of the initial amount of the photogenerated charge Q_0 and the electron mobility μ.

The electric field reconstruction starts from Eq. (2), whenever the transport parameters are known. To eliminate the parametric time dependence of the electric field as calculated from the Eq. (2), the low of motion at each applied voltage can be obtained:

$$x_i(t) = \int_0^t v_i(t')dt' = \mu \int_0^t E\left(x_i(t')\right)dt' \qquad (9)$$

In this way, it is possible to correlate each position with the related value of the electric field and then to reconstruct the spatial profile of electric field $E(x)$.

The transport parameters, electron mobility and lifetime, obtained for all investigated samples are summarized in Table II. Their product $(\mu\tau)_{TCT}$ for each sample has been compared with the product $(\mu\tau)_{CCE}$ obtained from Charge Collection Efficiency measurements, to check the validity of our procedure. CCE curves shown in Fig. 6 (open circles) have been fitted with different analytical models based on the assumption of uniform (Hecht) or linear [22] electric field profile, with and without surface recombination term [23]. The best fit for each curve has been obtained without surface recombination term and it is shown in Fig. 6 (solid lines). Mobility-lifetime products from TCT and CCE measurements are in excellent agreement. When the evaluation of the transport properties is requested, the novelty of the procedure here presented, with respect the well-known approach by means of the CCE measurements, is clearly the possibility to evaluate mobility and lifetime one by one.

Finally, the electric field profile along the sample thickness, as obtained from Eqs. (2) and (9), is shown in Fig. 7 for some representative applied voltages. The reconstructed electric field in samples A, C, and D show a uniform profile. Only in the sample B the electric field shows a linear increasing profile, in agreement with the fitting results of the CCE measurements (see Table II) giving a similar slope $|\alpha|$. The non-uniformity of the electric field is a signal of the presence of space charge. In fact, since the divergence of the electric field is proportional to the charge density, the presence of a linearly increasing field is due to a uniform density of negative localized charge equal to about $10^{11\div12}$ cm^{-3}. It must be emphasized that sample B has been grown with a different method.

To check the self-consistence of the proposed model, the areas below the curves in Fig. 4 were always calculated and the consistence with the real values of applied voltage has been verified to be within 5%.

The reconstruction of the electric field suffers, however, from artifacts in proximity of the electrodes for two different reasons. Since the profile of the field has been deduced from the current transient curves, the electric field near the cathode could be affected by light excitation that is not completely removed from the laser pulse deconvolution. The behavior below the cathode is surely affected by the presence of the metal and by the instantaneous carrier cloud generation too. We cannot exclude the presence of a high space charge related to the interfacial defectiveness of the material. Near the anode, the field shows instead a drop due to the carrier diffusion. The entity of these effects is strictly dependent on the transit time, but they are limited to a region near the contacts with an extension lower than 5% of the thickness of samples.

The excellent agreement between results of two independent experimental investigations on the same set of samples suggests the validity of the procedure here proposed. This means that thanks to the new method, the electric field profile inside the

samples can be determined together with transport properties, without any starting assumptions.

Sample	L (mm)	μ_{TCT} ($cm^2\ V^{-1}$)	τ_{TCT} (ns)	$(\mu\tau)_{TCT}$ ($10^{-3}\ cm^2\ V^{-1}$)	$(\mu\tau)_{CCE}$ ($10^{-3}\ cm^2\ V^{-1}$)	E profile	$\lvert\alpha\rvert_{TCT}$ ($V\ cm^{-2}$)	$\lvert\alpha\rvert_{CCE}$ ($V\ cm^{-2}$)
A	0.27	1040 ± 40	410 ± 30	0.43 ± 0.04	0.51 ± 0.06	uniform	-	-
B	0.50	1170 ± 60	510 ± 40	0.60 ± 0.05	0.65 ± 0.05	linear	600 ± 50	700 ± 100
C	2.50	1020 ± 40	980 ± 30	1.0 ± 0.1	1.1 ± 0.3	uniform	-	-
D	4.00	1050 ± 30	960 ± 40	1.0 ± 0.1	0.9 ± 0.1	uniform	-	-

Table II. Transport parameters and electric field feature of samples in Table I. Mobility-lifetime products from laser induced Transient Current Technique (TCT) and Charge Collection Efficiency (CCE) measurements for all the investigated samples are compared in the fifth and the sixth columns. The analytical model giving the best fit on the CCE curves appears in the column labelled as "*E* profile". For a linear profile of the electric field, the CCE curves have been analyzed following the model presented in Ref. [22]. The value of |α| represents the slope of the electric field profile.

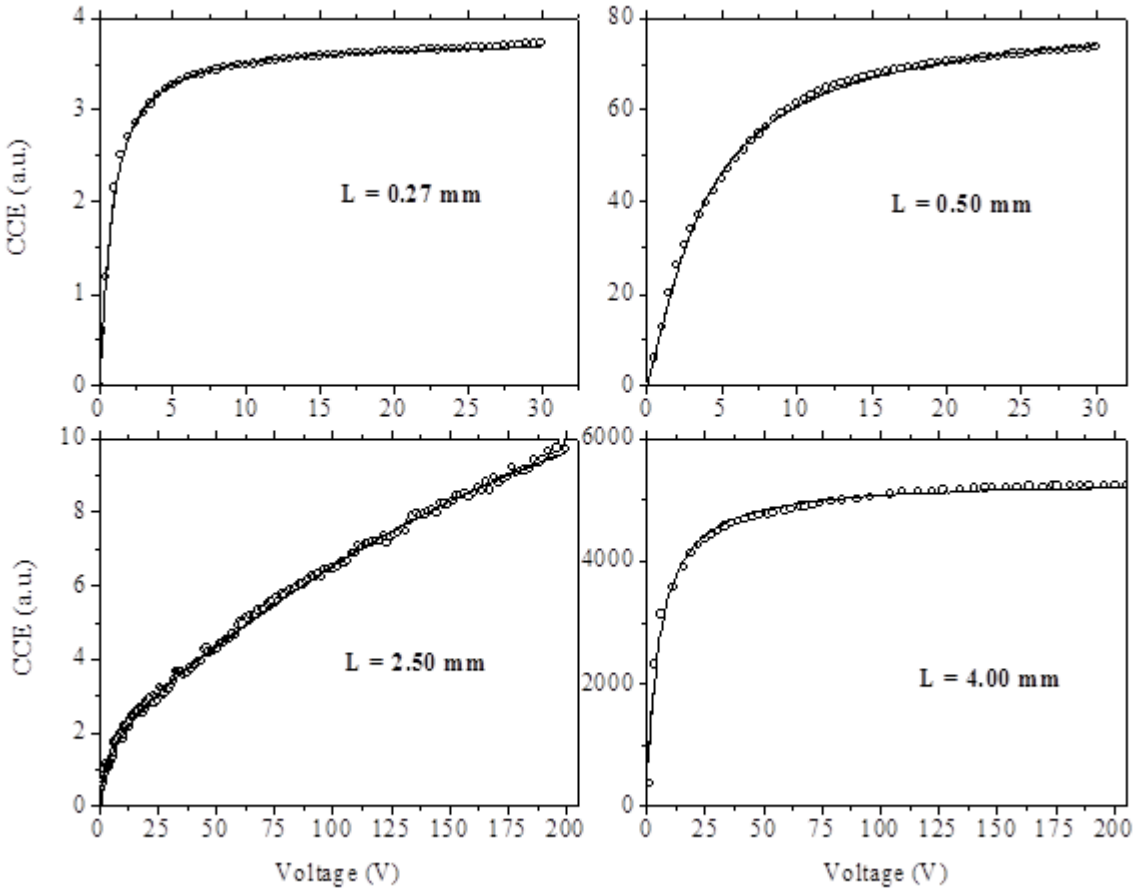

Fig. 6. Charge Collection Efficiency curves of samples in Table I as a function of the applied voltage, for an exciting photon beam at 790 nm (open circles). The solid lines are fits with the analytical electric field profile given in Table II.

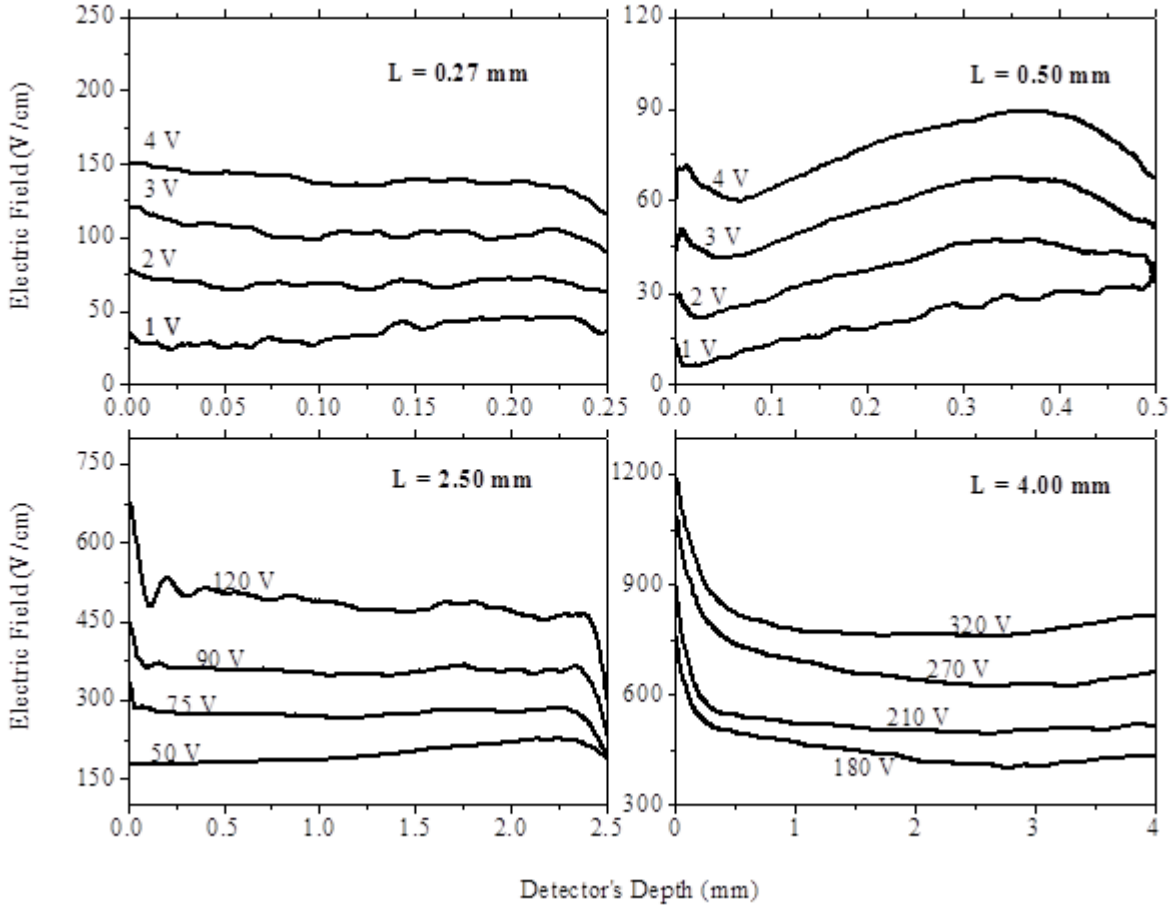

Fig. 7. Electric field spatial profiles as result of reconstruction from electronic TCT transients.

V. CONCLUSIONS

The spectroscopic features of bulk devices for high energy photon detection are strictly related to the charge transport properties of the active material and to the presence of space charge. The measure of the carrier mobility and lifetime is then of great interest together with the study of the electric field profile inside the volume of the detector.

A method based on TCT measurements, previously employed only in CdTe devices, has been tested on a set of CZT planar detectors with different thicknesses to evaluate the electron mobility and lifetime and to create a map of the electric field profile along the thickness of sample. The Ramo-Shockley theorem allows to link the electric field, experienced locally by the electron during its drift, with the shape of the current transient induced by the laser pulse. A minimization procedure, enables the evaluation of the electron lifetime and consequently of the electron mobility. Finally, the electric field inside the sample has been reconstructed by means of the law of motion.

Unlike previous methods based on current transients, no initial hypothesis on the shape of the electric field has been assumed. This method neglects the effects of diffusion and de-trapping, but improvements taking into account these effects are in progress. The procedure has demonstrated however its applicability in a set of CZT planar detectors those thickness ranges from 250 μm to 4 mm, and has yielded results in excellent agreement with results based on CCE measurements. Electron mobility and lifetime, obtained in this way, are at the state of art if compared with those in literature [10], [11], [24]. The presence of a negative space charge has been evidenced in only one sample and its density has been estimated.

Finally, a snapshot of the electric field profile inside CZT samples has been presented.

REFERENCES

[1] A. Cola, I. Farella, A.M. Mancini, and A. Donati, "Electric Field Properties of CdTe Nuclear Detectors", *IEEE Trans. Nucl. Sci.*, vol. 54, no. 4, pp. 868-872, Aug. 2007.

[2] P.J. Sellin, G. Prekas, J. Franc, and R. Grill, "Electric field distributions in CdZnTe due to reduced temperature and X-ray irradiation", *Appl. Phys. Lett.*, vol. 96, Apr. 2010, Art. no. 133509.

[3] J. Franc *et al.*, "Influence of contacts on electric field in an Au/(CdZn)Te/Au detector: a simulation", *IEEE Trans. Nucl. Sci.*, vol. 57, no. 4, pp. 2349-2358, Aug. 2010.

[4] A. Milani, B. Enrico, A. Zappettini, S.M. Pietralunga, and M. Martinelli, "Characterization of electro-optic shielding effect in bulk CdTe:In crystals", *J. Crystal Growth*, vol. 214, pp. 913-917, 2000.

[5] M. Strassburg, C. Schroeter, and P. Hackenschmied, "CdTe/CZT under high flux irradiation", *J. Instr.*, vol. 6, Jan. 2011, Art. no. C01055.

[6] L. Marchini *et al.*, "Crystal defects and charge collection in CZT x-ray and gamma detectors", *Conf. Rec 2010 IEEE Nucl. Sci. Symp.* (NSS/MIC), pp. 3674–3677.

[7] D. S. Bale, "Fluctuations in induced charge introduced by Te inclusions within CdZnTe radiation detectors", *J. Appl. Phys.*, vol. 108, Jul. 2010, Art. no. 024504.

[8] R.O. Pak and K.C. Mandal, "Defect Levels in Nuclear Detector Grade $Cd_{0.9}Zn_{0.1}Te$ Crystals Electronic Materials and Processing", ECS *J. Solid State Sci. Technol.* Vol. 5, no. 4, pp. P3037-P3040, 2016.

[9] M. Pavesi *et al.*, "On the role of boron in CdTe and CdZnTe crystals", *J. of Electronic Materials*, vol. 40, no. 10, pp. 2043-2050, Jul. 2011.

[10] S. Uxa, E. Belas, R. P. Grill, P. Praus, and R. B. James, "Determination of electric-field profile in CdTe and CdZnTe detectors using transient-current technique", *IEEE Trans. Nucl. Sci.*, vol. 59, no. 5, pp. 2402-2408, Oct. 2012.

[11] J. Fink, H. Krüger, P. Lodomez, and N. Wermes, "Characterization of charge collection in CdTe and CZT using the transient current technique", *Nucl. Instr. Meth. Phys. Res. A*, vol. 560, pp. 435-443, Feb. 2006.

[12] A. Santi *et al.*, "An original method to evaluate the transport parameters and reconstruct the electric field in solid-state photodetectors", *Appl. Phys. Lett.*, vol. 104, May 2014, Art. no. 193503.

[13] M. Zanichelli *et al.*, "Characterization of bulk and surface transport mechanisms by means of the photocurrent technique", *IEEE Trans. Nucl.Sci.*, vol. 56, no. 6, pp. 3591-3596, Dec. 2009.

[14] A. Zappettini *et al.*, "Boron oxide encapsulated vertical Bridgman grown CdZnTe crystals as X-Ray detector material", *IEEE Trans. Nuc.Sci.*, vol. 56, no. 4, pp. 1743-1746, Aug. 2009.

[15] A. Zappettini, M. Zha, M. Pavesi, and L. Zanotti, "Boron oxide fully encapsulated CdZnTe crystals grown by the vertical Bridgman technique", *J. Crystal Growth*, vol. 307, pp. 283-288, Jul. 2007.

[16] A. Zappettini *et al.*, "A new process for synthesizing high-purity stoichiometric cadmium telluride", *J. Crystal Growth*, vol. 214, pp. 14-18, 2000.

[17] M. Zha, F. Bissoli, A. Zappettini, G. Zuccalli, L. Zanotti, and C. Paorici, "Heat treatment in semi-closed ampoule for obtaining stoichiometrically controlled cadmium telluride" *J. Crystal Growth.*, vol. 237, pp. 1720-1725, Apr. 2002.

[18] M. Prokesch and C. Szeles, "Accurate measurement of electrical bulk resistivity and surface leakage of CdZnTe radiation detector crystals", *J. Appl. Phys.*, vol. 100, Jul. 2006, Art. no. 014503.

[19] L. Marchini *et al.*, "Study of surface treatment effects on the metal-CdZnTe interface", *IEEE Trans. Nucl. Sci.*, vol. 56, no. 4, pp. 1823-1826, Aug. 2009.

[20] W. Shockley, "Currents to conductors induced by a moving point charge", *J. Appl. Phys.*, vol. 9, pp. 635-636, May 1938.

[21] S. Ramo, "Currents Induced by Electron Motion", *Proc. of I.R.E.*, vol. 27, pp. 584-5g85, Apr. 1939.

[22] M. Zanichelli, A. Santi, M. Pavesi, and A. Zappettini, "Charge collection in semi-insulator radiation detectors in the presence of a linear decreasing electric field", *J. Phys. D: Appl. Phys.*, vol. 46, Jul. 2013, Art. no. 365103.

[23] A. Many, "High-field effects in photoconducting cadmium sulphide" 1965 *J. Phys. Chem. Solids*, vol. 26, no. 3, pp. 575-578, Mar. 1965.

[24] H.Y. Cho, J.H. Lee, Y.K. Kwon, J.Y. Moon, and C.S. Lee, "Measurement of the drift mobilities and the mobility-lifetime products of charge carriers in a CdZnTe crystal by using a transient pulse technique", *J. Inst.*, vol. 6, Jan. 2011, Art. no. C01025.

Maura Pavesi is Research Associate with the Dept. of Mathematical, Physical and Computer Sciences in Parma, (Italy). She worked on failure mechanisms and reliability of semiconductor devices. At the present, her activity is focused on the electro-optical characterization of wide-gap semiconductors and materials for X and Gamma-ray detection.

Andrea Santi is PhD student at Department of Physics and Earth Sciences, at the University of Parma, Italy. He got master degree on the opto-electronic characterization on CZT. At present he is working at the study of the carriers' transport and electric field on CZT-based detectors.

Manuele Bettelli is PhD student at the Institute of Materials for Electronics and Magnetism (IMEM), a public research institute of CNR (National Research Council) in Parma, Italy. He got master degree on the characterization of metal contacts on CZT. He is working at the development of high performance CZT-based detectors.

Andrea Zappettini is senior researcher at at the Institute of Materials for Electronics and Magnetism (IMEM), a public research institute of CNR in Parma, Italy. At IMEM he is head of the SIGNAL group, mainly concerned on the development of CZT-based X-ray detectors. He is author of 185 scientific papers on international journals, and author of 9 international patents.

Massimiliano Zanichelli between the beginning of June 2007 and the end of April 2008 worked as optical laboratory manager and problem solver in a factory for industrial and security. Since May 2008, he worked full time in the University of Parma for his Ph.D. program, dealing with semi-insulator transport properties, photocurrent techniques, and read-out electronics for CZT detectors.